Mixing and CP Violation at D0

G.A. Garcia-Guerra [a] on behalf of the D0 Collaboration

[a]Departamento de Física, CINVESTAV, AP 14-740, 07000 Mexico DF, Mexico

We present several mixing and CP violation measurements utilizing up to 2.8 fb^{-1} of proton-antiproton collisions collected by the D0 experiment at the Fermilab Tevatron. The achieved precision of some of these measurements is of the same level as the expected deviation predicted by some extensions of the Standard Model. One result suggests a tantalizing hint of new physics.

1. Introduction

A basic motivation for the study of the mixing quantities is to determine the standard model (SM) parameters and the search for new physics. For the former, the measurement of the $B_s^0 - \bar{B}_s^0$ oscillation frequency ΔM_s and the decay width difference $\Delta\Gamma_s$ are crucial for the determination of some elements of the CKM matrix [1]. For the latter, the CP-violating mixing phase ϕ_s is one of the most important parameters in the search of new physics, since the SM predicts a small value for this parameter [2], but recent measurements of this parameter suggests a hint of physics beyond the SM. Besides the B_s^0 system, the study of the decay $B^+ \to J/\psi K^+$ can also give us information about CP violation in this decay. The analyses reported in this proceedings were based on approximately 2.8 fb^{-1} of data recorded with the D0 detector [3] in $p\bar{p}$ collisions at $\sqrt{s} = 1.96$ TeV. All the D0 Conference Notes referred to in this document can be found in [4]. Unless it is explicitly stated, the appearance of a specific charge state will also imply its charge conjugate throughout.

2. B_s^0 mixing

2.1. Flavor tagging

A necessary step in the B_s^0 oscillation analysis is the determination of the $B_s^0/\bar{B}_s^0$ initial- and final-state flavors. The flavor of the B_s^0 at production is determined using both opposite- and same-side flavor tagging techniques. Some of the important parameters for describe the tagging performance are the purity ($\eta_s = N_{\text{correctly tagged events}}/N_{\text{total tagged events}}$), the dilution ($\mathcal{D} = 2\eta_s - 1$), the tagging efficiency ($\epsilon = N_{\text{total tagged events}}/N_{\text{total events}}$), and the tagging variable d_{tag} which is positive (negative) when an event is tagged as a b ($\bar{b}$) quark (see Ref. [5] for more details).

The opposite-side tagging (OST) of the initial flavor of the B_s^0 meson, which exploits the presence of a muon or an electron and/or a secondary vertex on the opposite side, is described elsewhere [6,7]. The same-side tagging (SST) technique uses the properties of the particles produced in association with the reconstructed B_s^0 meson. A combined OST+SST tagger is also used. The combination is done as follows [6,7]: For the events where OST is not defined, we add an opposite-side flavor tagger and combine it with SST. If both an OST and a SST are present, we combine them assuming they are independent. The total combined tagging power is $\epsilon\mathcal{D}^2 = (4.49 \pm 0.088)\,\%$. This is larger than the individual tagging powers of SST and OST.

2.2. The Flavor Oscillation Frequency of B_s^0 Mesons.

Neutral B_s^0 mesons mix with their antiparticles leading to oscillations between the flavor eigenstates. These oscillations are governed by the Schrödinger equation [2]

$$i\frac{d}{dt}\begin{pmatrix} |B_s^0(t)\rangle \\ |\bar{B}_s^0(t)\rangle \end{pmatrix} = \left(\mathbf{M} - \frac{i}{2}\mathbf{\Gamma}\right)\begin{pmatrix} |B_s^0(t)\rangle \\ |\bar{B}_s^0(t)\rangle \end{pmatrix}, \quad (1)$$

where $\mathbf{M}$ and $\mathbf{\Gamma}$ are the mass and decay matrices, respectively. The flavor oscillation frequency ΔM_s of the $B_s^0 - \bar{B}_s^0$ system is related with the elements of the mass matrix by means of the expression $\Delta M_s = M_H - M_L = 2|M_{12}|$. M_L and M_H are the masses of the physical light (L) and heavy (H) eigenstates $|B_s^L\rangle$ and $|B_s^H\rangle$. Since the matrix element M_{12} is related some elements of the CKM matrix, the measurement of ΔM_s can be used as an important test of the SM, which predicts a value for the oscillation frequency to be (19.3 ± 6.7) ps^{-1} [2]. Currently, the Tevatron is currently the only place where it is possible to make this measurement [5,8].

The final states for the B_s^0 mesons considered in this analysis and the total number of D_s^- candidates after we apply the cuts [7] are summarized in Table 1.

Table 1
Signal candidates for the decays under study.

Decay mode	N_{sig}
$B_s^0 \to \mu\nu D_s(\phi\pi)X$	$44,777 \pm 415$
$B_s^0 \to e\nu D_s(\phi\pi)X$	$1,663 \pm 102$
$B_s^0 \to \mu\nu D_s(K^{*0}K)X$	$18,098 \pm 903$
$B_s^0 \to \pi D_s(\phi\pi)X$	249 ± 17
$B_s^0 \to \mu\nu D_s(K_s^0 K)X$	593 ± 67

In order to take into account the effects of undetected neutrinos present in the semileptonic decays and the non-reconstructed charged particles in the partially reconstructed hadronic- and semileptonic decays, we scale the measured momentum of the B candidate by a factor $K = p_T\,(l(\pi)D_s)\,/p_T(B)$, estimated from MC simulation, where p_T denotes the perpendicular momentum to the beam. Fig. 1 shows the K factor distributions for the semi-muonic decays of the B_s^0 meson.

For both the semileptonic and hadronic decays, the probability density functions are described in detail in Ref. [7]. To obtain the final D0 measurement for the oscillation frequency, we combine the individual amplitude scans for each of the modes in Table 1 into a single amplitude scan. After this, the scan is translated to a likelihood using the relationship between the fitted amplitude at a scan point ΔM_s, its error, and the difference between the log-likelihood at that point and the log-likelihood at infinity: $\Delta\mathcal{L} = (1/2 - \mathcal{A}_{\rm fit}(\Delta M_s))/\sigma^2_{\mathcal{A}}$. Both the combined amplitude and the likelihood scans are shown in Fig. 2. The systematic uncertainties that contribute in a significant way for most of the channels reported in Table 1 are the OST dilution uncertainty, the $K-$factor resolution, and the sample composition [7].

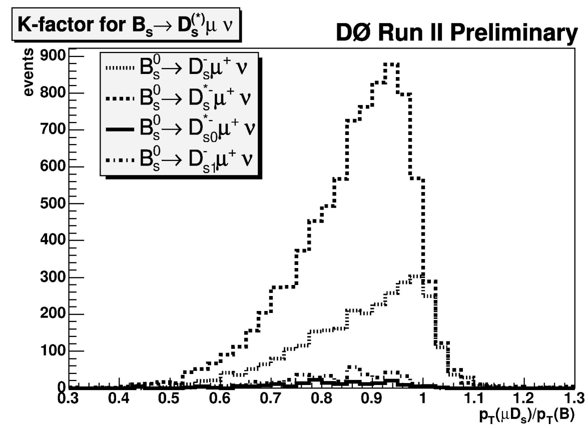

Figure 1. K factor distributions for the semi-muonic decays of the B_s^0 meson

The D0 measurement for the oscillation frequency is

$$\Delta M_s = 18.53 \pm 0.93\,(\rm stat) \pm 0.30\,(\rm syst)\,\rm ps^{-1}. \quad (2)$$

This value is consistent with the theoretical prediction [2] and the CDF measurement [8]. The significance of this measurement, ${\rm Sig}(\sigma) = \sqrt{-2\Delta\ln\mathcal{L}}$, including systematic uncertainties is 2.9σ.

3. CP violation in the decay $B_s^0 \to J/\psi\phi$

The other two important parameters related with the eq. (1) are the CP-violating mixing phase ϕ_s and the decay width difference $\Delta\Gamma_s \equiv \Gamma_L - \Gamma_H = 2|\Gamma_{12}|\cos\phi_s$, where Γ_L and Γ_H are the

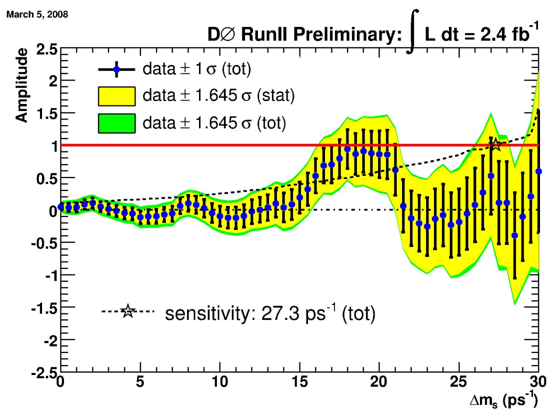

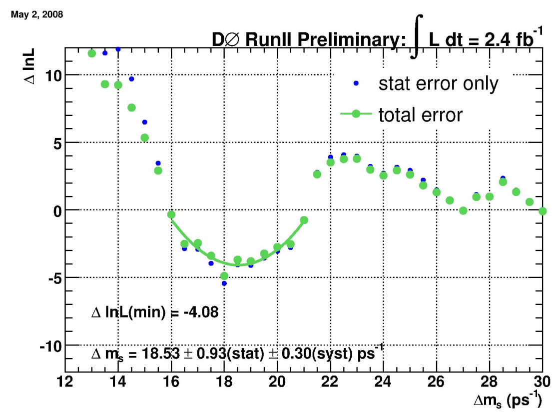

Figure 2. Left: The combined amplitude scan for the channels reported in Table 1. Right: The combined likelihood scan derived from the combined amplitude fit values. Values of $\Delta \ln \mathcal{L}$ using both statistical (small points) and total uncertainties (large points) are shown as is the parabolic fit.

decay rates for the same eigenstates as in subsection 2.2. In the SM, the phase ϕ_s and the decay width $\Delta\Gamma_s$ are predicted to be -0.04 ± 0.01 rad and 0.088 ± 0.017 ps^{-1} respectively. Previously [9], D0 reported a measurement of this CP-violating phase on the decay chain $B_s^0 \to J/\psi\phi$, $J/\psi \to \mu^+\mu^-$, $\phi \to K^+K^-$. Here we present recent D0 results [10] on the CP-violating phase and the decay width difference in the same decay channel by including information on the B_s^0 flavor at the production time using the techniques reported in subsection 2.1 in order to improve the precision of the measurement.

After all the cuts [9,10] are applied, we perform an unbinned maximum likelihood to fit the proper decay time, the three decay angles characterizing the final state in the transversity basis [11], and the mass of the 48,047 candidates, whose invariant mass distribution is shown in Fig. 3.

The likelihood function $\mathcal{L}$ is given by

$$\mathcal{L} = \prod_{i=1}^{N} \left[f_{\rm sig}\mathcal{F}^i_{\rm sig} + (1 - f_{\rm sig})\mathcal{F}^i_{bkg} \right] , \qquad (3)$$

where N is the total number of events and $f_{\rm sig}$ is the fraction of the signal in the sample. The function $\mathcal{F}^i_{\rm sig}(\mathcal{F}^i_{\rm bkg})$ describes the distribution of the signal (background) in the mass, proper decay time, and decay angles [10]. The time evolution of the angular distribution of the decay products in the transversity basis and its dependence on $\Delta M_s, \phi_s, \Delta\Gamma_s$, the relative strong phases δ_1 and δ_2, and the magnitudes of the amplitudes $|A_0|, |A_\parallel|$, and $|A_\perp|$ is given in Ref. [10,11]. The

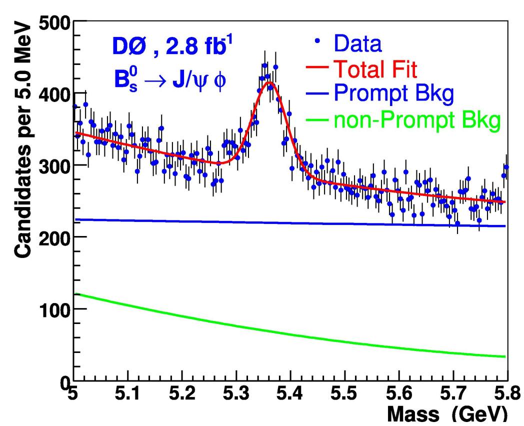

Figure 3. Invariant mass distribution of the B_s^0 system. The curves correspond to the projections of the maximum likelihood fit. The fit assigns $1,967 \pm 65\,$(stat) events to the B_s^0 decay.

amplitudes correspond to the longitudinal, parallel, and perpendicular components, respectively, to the linear polarization states of the vector mesons J/ψ and ϕ.

For a given event, the decay rate is the sum of the B_s^0 and $\bar{B}_s^0$ rates weighted by P(B_s^0) and 1-P(B_s^0), respectively, and by the detector acceptance. P(B_s^0) is the related probability of having a pure state B_s^0 at $t = 0$.

Due to the high degree of correlation between $\Delta M_s, \phi_s, \delta_1$, and δ_2 we cannot obtain stable fits when all the parameters of the fit are allowed to float. In the following, we fix ΔM_s to 17.77 ± 0.12 ps^{-1}, as measured in Ref. [8] and allow the phases δ_i to vary around the world-average values [12] for the $B_d^0 \to J/\psi K^{*0}$ decay, $\delta_1 = -0.46$ and $\delta_2 = 2.92$, under a Gaussian constraint with a width of $\pi/5$. This is to allow some degree of violation of the $SU(3)$ symmetry relating the two processes.

We have no evidence of significant bias from the studies using pseudo-experiments with similar statistical sensitivity. We estimate the systematic uncertainties due to the flavor-tagging purity by varying its parametrization within uncertainties. An interference term is introduced in the background model. The difference between fits with and without this term is considered as the systematic uncertainty associated with the background model. Confidence level contours in the $\phi_s - \Delta\Gamma_s$ plane and the likelihood profile as a function of ϕ_s are shown in Fig. 4. The final results are reported in Table 2.

Table 2
Final measurements for the angular and time parameters of the decay $B_s^0 \to J/\psi\phi$. The first uncertainty is statistical and the second systematic.

Parameter	Measurement
$\bar{\tau}_s$ (ps)	$1.52 \pm 0.06 \pm 0.01$
$\Delta\Gamma_s$ (ps^{-1})	$0.19 \pm 0.07^{+0.02}_{-0.01}$
$A_\perp(0)$	$0.41 \pm 0.04^{+0.01}_{-0.02}$
$\lvert A_0(0)\rvert^2 - \lvert A_\parallel(0)\rvert^2$	$0.34 \pm 0.05 \pm 0.03$
ϕ_s (rad)	$-0.57^{+0.24+0.07}_{-0.30-0.02}$
ΔM_s (ps^{-1})	$\equiv 17.77$

These results supersede the previous measurements [9] that were based on the untagged decay $B_s^0 \to J/\psi\phi$ and a smaller data sample.

4. $\Delta\Gamma_s$ from Br($B_s^0 \to D_s^{(*)} D_s^{(*)}$)

As pointed out in section 3 in the SM the $B_s^0 - \bar{B}_s^0$ mixing phase ϕ_s is expected to be small. However, in the presence of new physics, the CP-violating phase ϕ_s can be large and $\Delta\Gamma_s$ is diminished by a factor of $\cos\phi_s$; $\Delta\Gamma_s = \Delta\Gamma_s^{CP}\cos\phi_s$, where $\Delta\Gamma_s^{CP} = \Gamma_s^{even} - \Gamma_s^{odd}$. A value for this parameter can be extracted by measuring the Br($B_s^0 \to D_s^{(*)} D_s^{(*)}$) under some theoretical assumptions where the decay $B_s^0 \to D_s^{(*)} D_s^{(*)}$ becomes CP-even to within 5% [13]. The relation between the branching ratio and $\Delta\Gamma_s^{CP}$ is the following

$$2\mathrm{Br}(B_s^0 \to D_s^{(*)} D_s^{(*)}) \simeq \Delta\Gamma_s^{CP}\left[\frac{1+\cos\phi_s}{2\Gamma_L} + \frac{1-\cos\phi_s}{2\Gamma_H}\right]. \quad (4)$$

If we assume no new physics $\Delta\Gamma_s^{CP} \equiv \Delta\Gamma_s$. In this analysis, we considered B_s^0 decays into two $D_s^{(*)}$ mesons, where $D_s^{(*)}$ denotes either D_s or $D_s^{(*)}$, since we cannot distinguish between them because of the undetected particles in the $D_s^* \to D_s\gamma/\pi^0$ decay. We search for one $D_s^{(*)}$ decaying to $\phi\pi\,(\equiv \phi_1\pi)$ and the other decaying to $\phi\mu\nu\,(\equiv \phi_2\mu\nu)$, where both ϕ's decay to K^+K^-. The branching ratio measurement is performed by normalizing the $B_s^0 \to D_s^{(*)} D_s^{(*)}$ sample to the $B_s^0 \to D_s^{(*)}\mu\nu$ sample [14]:

$$R_1 = 2\mathrm{Br}(B_s^0 \to D_s^{(*)} D_s^{(*)}) R_2 R_3 \quad (5)$$

where

$$R_1 = \frac{N(B_s^0 \to D_s^{(*)} D_s^{(*)})}{N(D_s\mu) f(B_s^0 \to D_s^{(*)}\mu\nu)}$$

$$R_2 = \frac{\mathrm{Br}(D_s \to \phi\mu\nu)\mathrm{Br}(\phi \to KK)}{\mathrm{Br}(B_s^0 \to D_s^{(*)}\mu\nu)}$$

$$R_3 = \frac{\epsilon(B_s^0 \to D_s^{(*)} D_s^{(*)})}{\epsilon(B_s^0 \to D_s^{(*)}\mu\nu)}$$

Here N is the number of events in each sample, f is the fraction of events in the $D_s\mu$ sample origi-

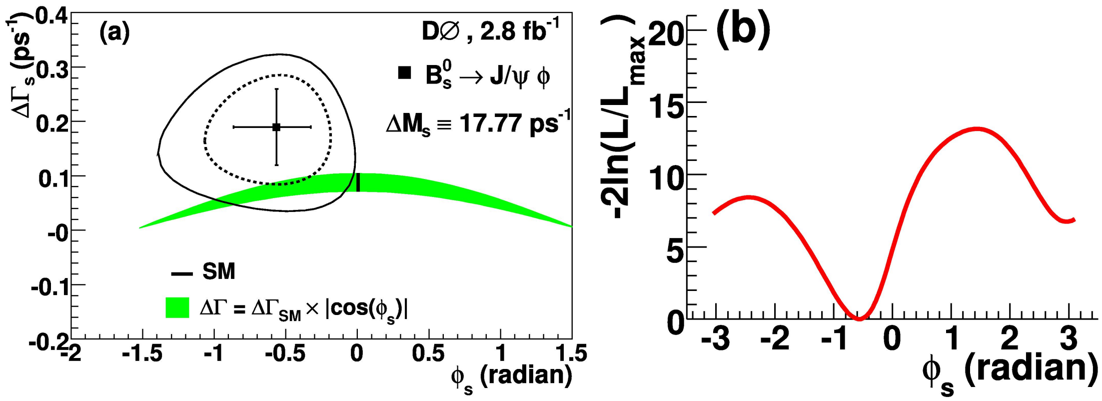

Figure 4. (a) Confidence-level contours in the $\Delta\Gamma_s - \phi_s$ plane. The curves correspond to the expected C.L.=68.3% (dashed) and 90% (solid). The cross shows the best fit point and one-dimensional uncertainties. Also shown is the SM predictions $\phi_s = -0.04$ rad and $\Delta\Gamma_s = 0.088 \pm 0.017$ ps^{-1}. (b) Likelihood profile of ϕ_s.

nating from the $B_s^0 \to D_s^{(*)}\mu\nu$ decay, and ϵ is the reconstruction efficiency.

After all the cuts [14] are applied, we choose a binned likelihood fit for the $D_s\mu$ sample. The resulting $D_s(\phi_1\pi)$ and $\phi_1(KK)$ invariant mass distributions are shown in Fig. 5. The fit gives $N(D_s\mu) = 28,680 \pm 288$ events. The reconstruction efficiency is estimated through a MC study. The resulting estimate of the ratio of reconstruction efficiencies R_3 is (8.7 ± 1.5)%. To obtain the factor R_2, we take the branching ratios from those reported in literature [15].

The main systematic uncertainty arises from the precision in the branching ratio measurements from Ref. [15]. They are allowed to vary within one standard deviation. $\mathrm{Br}(B_s^0 \to D_s^{(*)}\mu\nu)$ is the dominant source which gives around a 50% contribution to the total systematic uncertainty. Using all these inputs, we obtain the branching ratio from Eq. (5).

Assuming Eq. (4) is valid and allowing no new physics, we obtain

$$\frac{\Delta\Gamma_s}{\Gamma_s} = 0.088 \pm 0.030\,(\mathrm{stat}) \pm 0.036\,(\mathrm{syst}). \qquad (6)$$

This result is consistent with the theoretical prediction [2] and with previous measurements [12,16].

5. Direct CP violation in the decay $B^+ \to J/\psi K^+$

In the decay $B^\pm \to J/\psi K^\pm$ the charge asymmetry, defined as

$$A_{CP}\left(B^+ \to J/\psi K^+\right) =$$

$$\frac{N\left(B^- \to J/\psi K^-\right) - N\left(B^+ \to J/\psi K^+\right)}{N\left(B^- \to J/\psi K^-\right) + N\left(B^+ \to J/\psi K^+\right)}, \qquad (7)$$

is predicted to be small (~ 0.3%) by the SM [17]. Thus, a charge asymmetry observed at 1% or higher would indicate new physics.

The resulting invariant mass distribution, after all the cuts [18] are applied, is shown in Fig. 6.

In order to measure the charge asymmetry A between the $J/\psi K^+$ and $J/\psi K^-$ final states and to understood the possible differences between the positive and negative kaon production, we should take into account both physics and detector effects. One physics asymmetry is direct CP violation in the $B^+ \to J/\psi K^+$ decay. In addition, forward-backward charge asymmetry of events produced in the proton-antiproton collisions can also be present. The detector can give

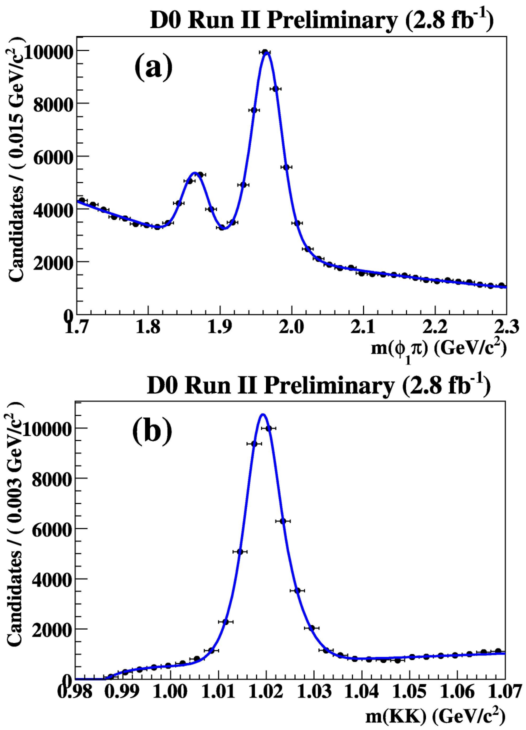

Figure 5. Invariant mass distributions for the $D_s\mu$ sample. (a) $m(\phi_1\pi)$ spectrum from the KK signal region. The two peaks represent the $D^\pm \to \phi\pi$ (left) and the $D_s \to \phi\pi$ (right). (b)$m(KK)$ spectrum from the $m(\phi_1\pi)$ signal region.

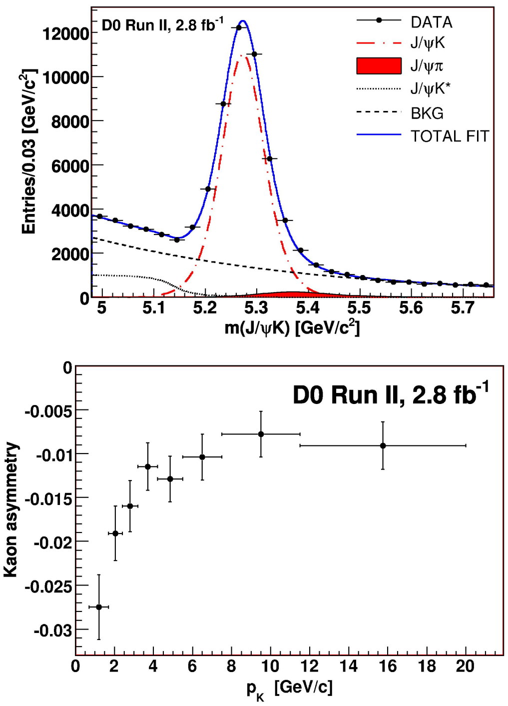

Figure 6. Top: The $J/\psi K$ invariant mass distribution. The curves correspond to the projections of the unbinned likelihood fit. The $B \to J/\psi K$ signal contains $40,222 \pm 242\,(\mathrm{stat})$ events. Bottom: Dependence of the kaon asymmetry on the kaon momentum p_K. Errors are statistical.

rise to an artificial asymmetries too. The magnet polarity can introduce a bias on the reconstruction efficiencies for the positive and negative kaons if it remains always in the same direction. So, all detector effects can be canceled by regularly reversing of the magnet polarity. This important feature is characteristic of the D0 detector [3].

The event sample of Fig. 6 is divided into eight subsamples corresponding to all possible combinations of the solenoid polarity $\beta = \pm 1$, the sign of the pseudorapidity of the $J/\psi K$ system $\gamma = \pm 1$, and the charge sign $q = \pm 1$ of the kaon candidate. The number of events $n_q^{\beta\gamma}$ of each subsample for the contributing channels $B_d^0 \to J/\psi K, J/\psi\pi$, and $J/\psi K^{*0}$ is obtained from a unbinned likelihood fit to the mass distribution of Fig. 6. The relation between $n_q^{\beta\gamma}$ and the charge asymmetry A under study is the following [18]:

$$\begin{aligned} n_q^{\beta\gamma} &= \frac{1}{4} N\epsilon^\beta\,(1+qA)\,(1+q\gamma A_{fb})\,(1+\gamma A_{\mathrm{det}}) \\ &\times\ (1+q\beta\gamma A_{q\beta\gamma})\,(1+q\beta A_{q\beta}) \\ &\times\ (1+\beta\gamma A_{\beta\gamma})\,, \end{aligned} \tag{8}$$

where N is the total number of signal events; ϵ^β is the fraction of integrated luminosity with solenoid polarity $\beta\,(\epsilon^+ + \epsilon^- = 1)$; A_{fb} accounts for possible forward-backward asymmetric B meson production; A_{det} is the detector asymmetry for kaons emitted in the forward and backward direction; $A_{q\beta\gamma}$ accounts for the change in acceptance of kaons of different sign bent by the solenoid in different directions; $A_{q\beta}$ is the detector asymmetry, which accounts for the change in the kaon reconstruction efficiency when the solenoid polarity is reversed; and $A_{\beta\gamma}$ accounts for any detector-related forward-backward asymmetries that remain after the solenoid polarity flip. To extract all the asymmetries, we perform a χ^2 to Eq. 8. The results are presented in Table 3.

Table 3
Physics and detector asymmetries for $J/\psi K$.

Asymmetry	Measurement
ϵ^+	0.506 ± 0.003
A	$-0.0070 + 0.0060$
A_{fb}	$0.0013 + 0.0060$
A_{det}	$-0.0033 + 0.0060$
$A_{q\beta\gamma}$	$-0.005 + 0.006$
$A_{q\beta}$	$0.0001 + 0.0060$
$A_{\beta\gamma}$	$-0.0030 + 0.006$

Another effect that should be taken into account is the difference in the interaction cross-section of the positive and negative kaons with the detector material [3,15]. The reaction $K^-N \rightarrow Y\pi$ (where Y are hyperons) has no K^+N analog arising in a kaon asymmetry that affects the charge asymmetry $A\,(B \rightarrow J/\psi K)$. This kaon asymmetry is measured in different bins of kaon momentum p_K as shown in Fig. 6. The obtained asymmetry is determined to be $A_K = 0.0145 \pm 0.0010$. The systematic uncertainty related with this asymmetry is found to be 0.0005.

The systematic uncertainty due to the shape of the $J/\psi K^{*0}$ contribution to the likelihood function (parameterized using the MC simulation) is found to be 0.0025. To obtain the systematic uncertainty from the unbinned fit of the mass distribution in Fig. 6 we vary the parameters fixed during the fitting in the $q\beta\gamma$ subsamples by $\pm 1\sigma$. This uncertainty is found to be 0.002. The systematic uncertainty from the choice of the fitting range is determined to be 0.004.

Finally, by taking into account the kaon asymmetry and the systematic uncertainties added in quadrature, the direct CP violation asymmetry in $B^+ \rightarrow J/\psi K^+$ is measured to be $A_{CP}\,(B^+ \rightarrow J/\psi K^+) = +0.0075 \pm 0.0061\,(\text{stat}) \pm 0.0027\,(\text{syst})$, which is consistent with the world-average value $+0.015 \pm 0.017$ [15], but has a factor of two improvement in precision.

6. Conclusions

The D0 Collaboration has been reporting new measurements and improving the existing ones in its broad physics program, especially on mixing and CP violation. In this proceedings, we report only some of the analysis related with these topics that are currently under study at D0. The increasing of data samples, the improvements in the detector, and the sophistication of the techniques such as the flavor tagging for the B_s^0 samples, allow us to measure parameters that are predicted by the SM such as the direct CP violation in the decay $B^+ \rightarrow J/\psi K^+$, the flavor frequency oscillation ΔM_s and the ratio $\Delta\Gamma_s/\Gamma_s$ of the $B_s^0 - \bar{B}_s^0$ system. In the other hand, in this system one of the measurements reported here, the CP-violating mixing phase ϕ_s, suggests a tantalizing hint on new physics.

7. Acknowledgments

This work was performed under the auspices of CONACyT Mexico and CINVESTAV Mexico City. The author want to thank the staffs at Fermilab and collaborating institutions.

REFERENCES

1. A. Lenz, in *Proceedings of the XI Mexican Workshop on Particles and Fields, Tuxtla Gutiérrez , Mexico, 2007*, edited by H. Castilla-Valdez, O. Miranda, and E. Santos. AIP Conf. Proc. vol. 1026. arXiv:0802.0977 (2008) [hep-ph].
2. A. Lenz, and U. Nierste, J. High Energy Physics **0706**, 072 (2007), arXiv:hep-ph/0612167.
3. V. Abazov *et al.* [D0 collaboration], Nucl. Instr. and Meth. A **565**, 463 (2006).

4. D0 public results. http://www-d0.fnal.gov/Run2Physics/WWW/results/b.htm
5. V. Abazov *et al.* [D0 Collaboration], Phys. Rev. Lett. **97**, 021802 (2006).
6. V. Abazov *et al.* [D0 Collaboration], Phys. Rev. D **74**, 112002 (2006).
7. D0 Collaboration, *A Search for B_s^0 Oscillations Using $B_s^0 \to D_s \mu X (D_s \to K_S^0 K)$ Decays.* D0 Conference Note 5254; *Measurement of the Flavor Oscillation Frequency of B_s^0 Mesons at D0.* D0 Conference Note 5474; *D0 B_s^0 oscillation combination for Summer 2007.* D0 Conference Note 5618.
8. A. Abulencia *et al.* [CDF Collaboration], Phys. Rev. Lett. **97**, 242003 (2006).
9. V. Abazov *et al.*, [D0 Collaboration], Phys. Rev. Lett. **98**, 121801 (2007).
10. V. Abazov *et al.*, [D0 Collaboration], arXiv:0802.2255 [hep-exp]. Submitted to Phys. Rev. Lett.
11. I. Dunietz, R. Fleischer, and U. Nierste, Phys. Rev. D **63**, 114015 (2001).
12. E. Barberio *et al.*, [Heavy Flavor Averaging Group], arXiv:0808.1297v1 [hep-ex].
13. I. Dunietz *et al.*, Phys. Rev. D **63**, 114015 (2001).
14. D0 Collaboration, *Measurement of Br($B_s^0 \to D_s^{(*)} D_s^{(*)}$) and the Lifetime Difference in the B_s^0 System.* D0 Conference Note 5651.
15. W. M. Yao *et al.*, [Particle Data Group], J. Phys. G **33**, 1 (2006) and 2007 partial update for edition 2008.
16. V. Abazov *et al.*, [D0 Collaboration], Phys. Rev. Lett. **99**, 241801 (2007).
17. W.-S. Hou, M. Nagashima and A. Soddu, arXiv:0605080 [hep-ph].
18. V. Abazov *et al.*, [D0 Collaboration], Phys. Rev. Lett. **100**, 211802 (2008).